

### **Conversion $K_{W/OM/G}$ to saturation concentration ( $C^*$ , $\mu\text{g}/\text{m}^3$ )**

According to Donahue et al. (2006),  $K_{org/G}$  can be converted to  $C_i^*$  through :

$$K_{org/G} = 1/C_i^*$$

Where  $K_{org/G}$  is partitioning coefficient between organic and gas phase in units of  $\text{m}^3$  (air) /  $\mu\text{g}$  (absorbing organics). If we assume the density of the absorbing organics is  $1 \text{ g}/\text{cm}^3$  (i.e.,  $10^{12} \mu\text{g}/\text{m}^3$ ), then the following should hold:

$$K_{W/OM/G} = K_{org/G} \cdot 10^{12} (\mu\text{g}/\text{m}^3) = 1/C^* \cdot 10^{12} (\mu\text{g}/\text{m}^3)$$

### **Conversion of $K_{W/G}$ to Henry's constant ( $K_H$ ) in unit $\text{M}/\text{atm}$**

Henry's constant ( $K_H$  in unit of  $\text{M}/\text{atm}$ ) can be converted to  $K_{W/G}$  according to the following relationship:

$$K_{W/G} = K_H \cdot R \cdot T$$

Where  $R$  is the gas constant in unit of  $\text{L atm K}^{-1} \text{ mol}^{-1}$  and  $T$  is temperature in  $\text{K}$ .

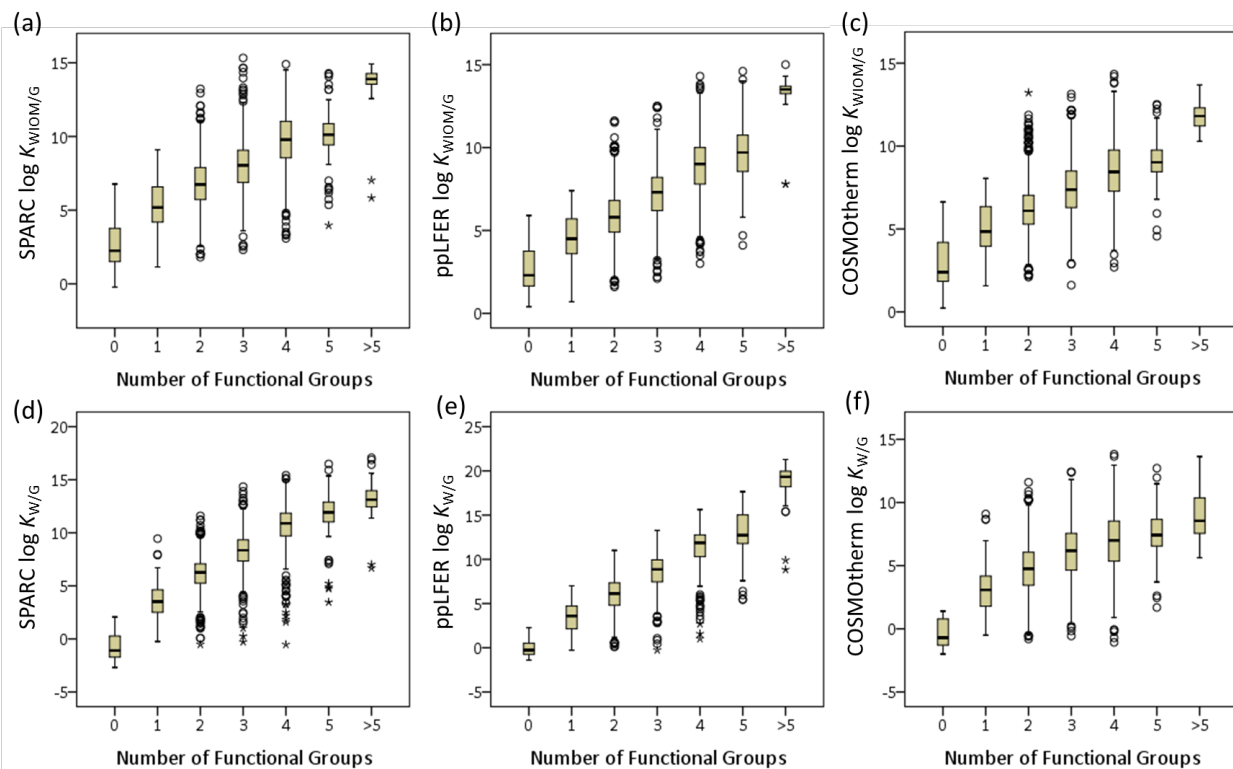


**Figure S1** Boxplot of log  $K_{WIOM/G}$  (upper panel) and log  $K_{W/G}$  (lower panel) for compounds with different number of functional groups. The line inside each box (and the number on the side) shows the median of log  $K_{WIOM/G}$  or log  $K_{W/G}$  for different categories of compounds. The marker circle and star indicates possible outliers and extreme values, respectively.

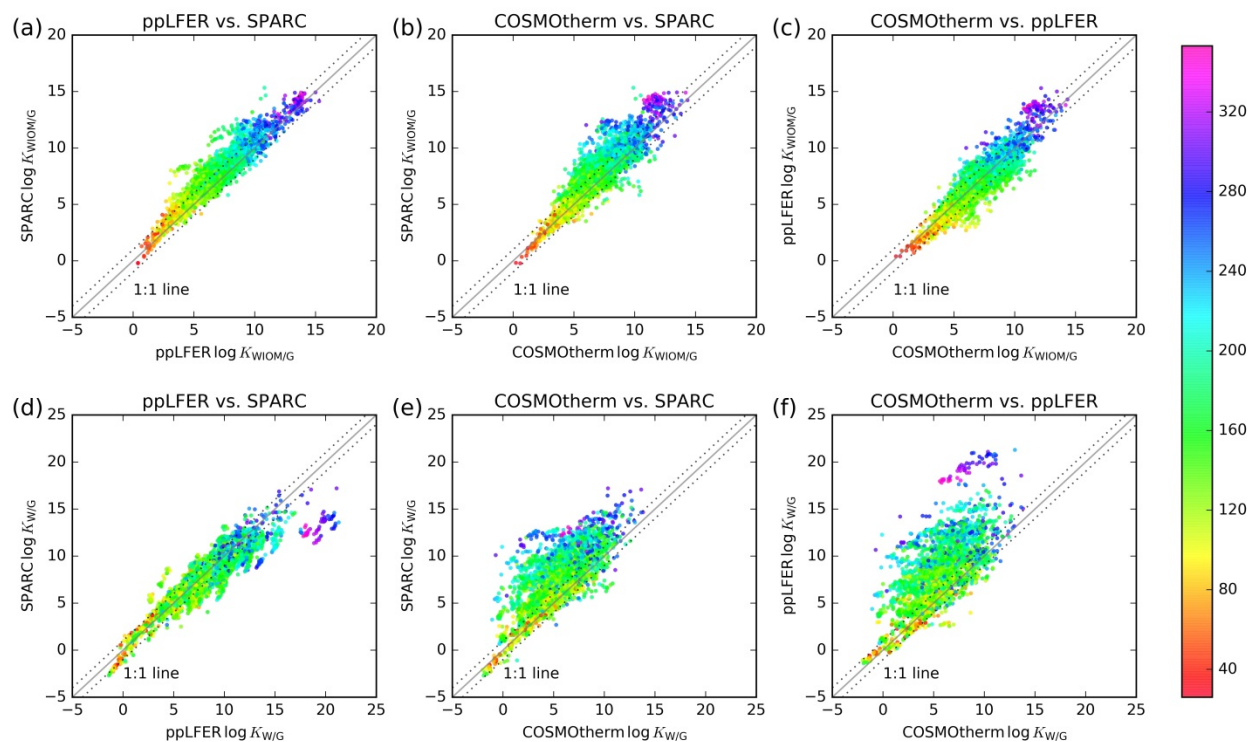


**Figure S2** Comparison of the  $K_{WIOM/G}$  (upper panel) and  $K_{W/G}$  (lower panel) predicted using COSMOtherm, SPARC and ppLFERs. The solid line indicates a 1:1 agreement. The dotted lines indicate the deviation by  $\pm 1$  log unit. The color scale indicates the molecular mass of the molecules (in units of g/mol).

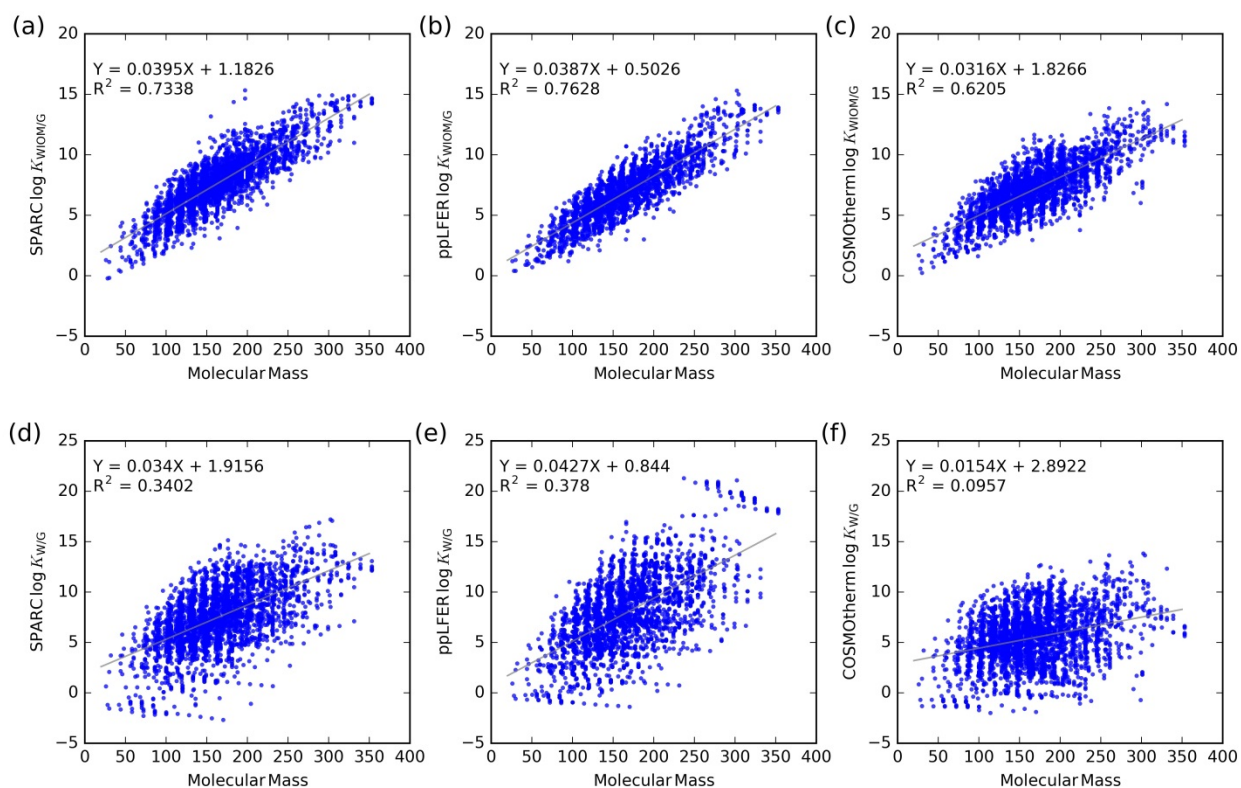


**Figure S3** Correlation of predicted  $K_{WIOM/G}$  (upper panel) and  $K_{W/G}$  (lower panel) with the molecular mass (in units of g/mol). The lines show the regressions of partitioning coefficients with molecular mass. Also shown are the regression equations.

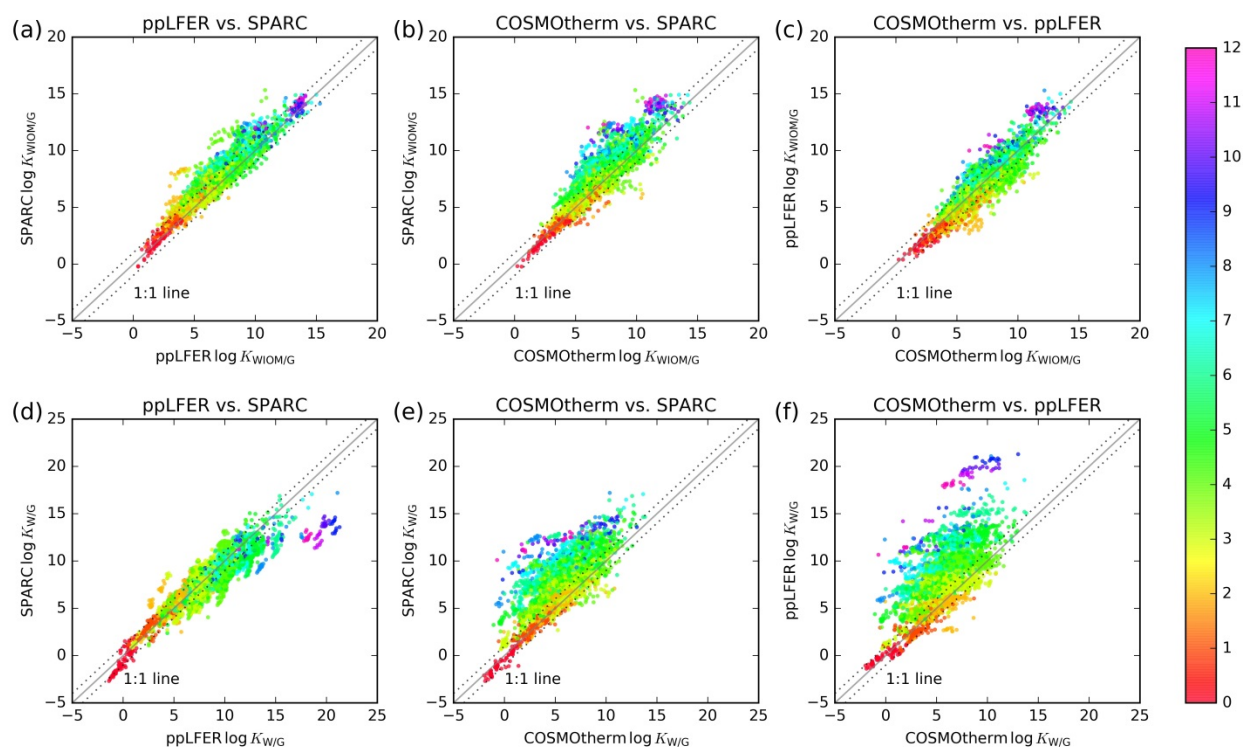


**Figure S4** Comparison of the  $K_{WIOM/G}$  (upper panel) and  $K_{W/G}$  (lower panel) predicted using COSMOtherm, SPARC and ppLFEr. The color scale indicates the number of oxygen in the molecules. The solid line indicates a 1:1 agreement. The dotted lines indicate the deviation by  $\pm 1$  log unit.

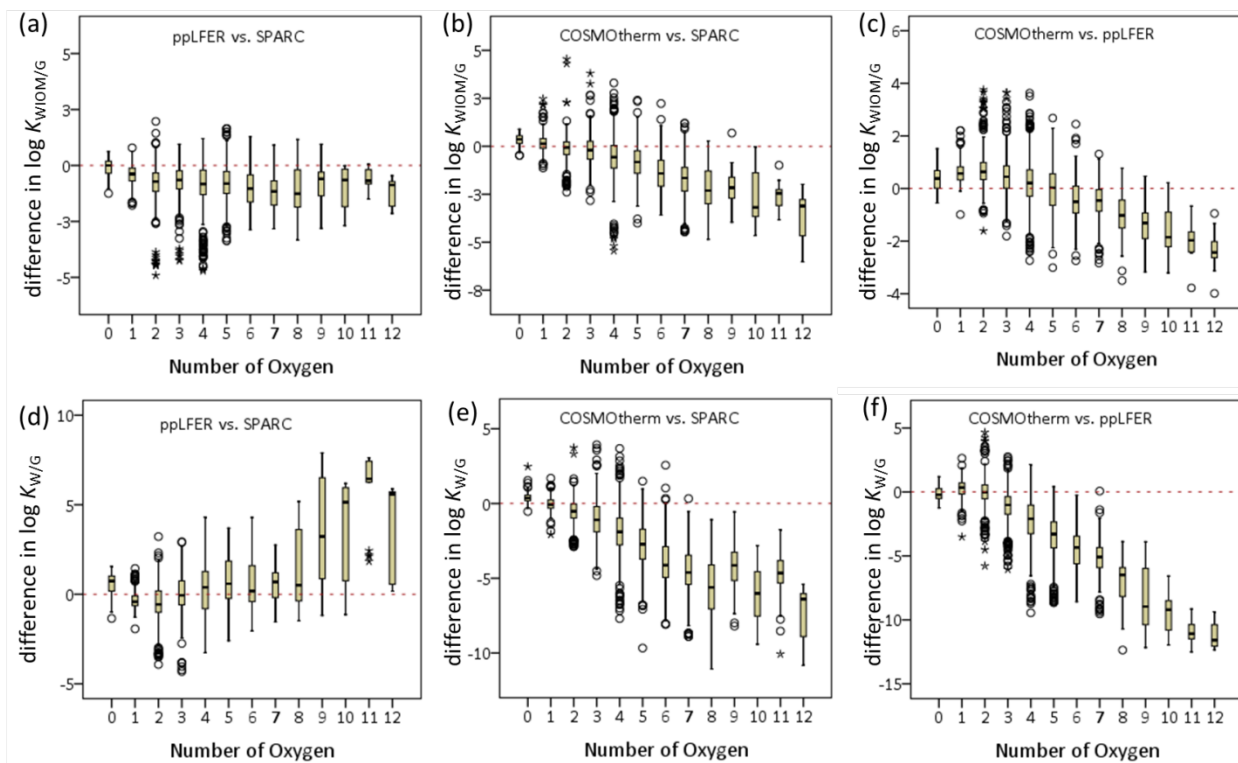


**Figure S5** Boxplot of difference in SPARC, ppLFEr and COSMOtherm predictions for compounds with different number of oxygens. The line inside each box shows the median difference for log  $K_{W/O/M/G}$  or log  $K_{W/G}$  for different categories of compounds. The marker circle and star indicates possible outliers and extreme values, respectively.

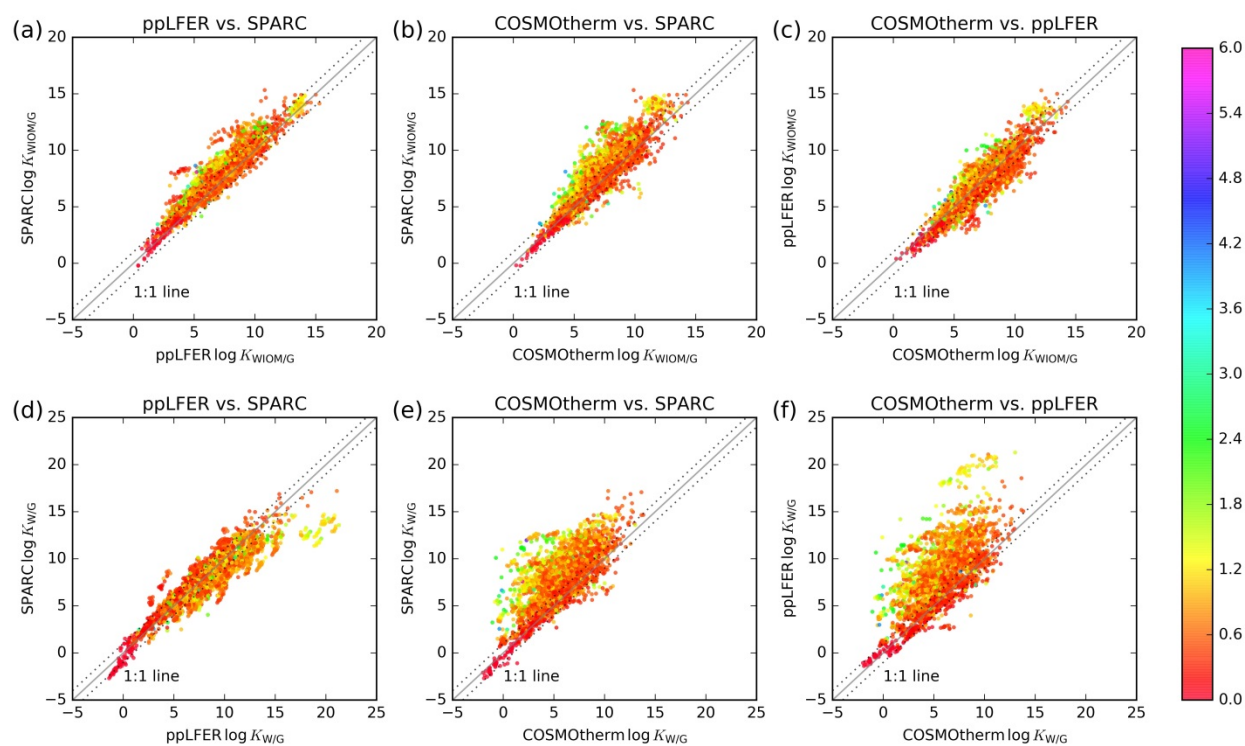


**Figure S6** Comparison of the  $K_{WIOM/G}$  (upper panel) and  $K_{W/G}$  (lower panel) predicted using COSMOtherm, SPARC and ppLFEr. The color scale indicates the O:C ratio of the molecules.

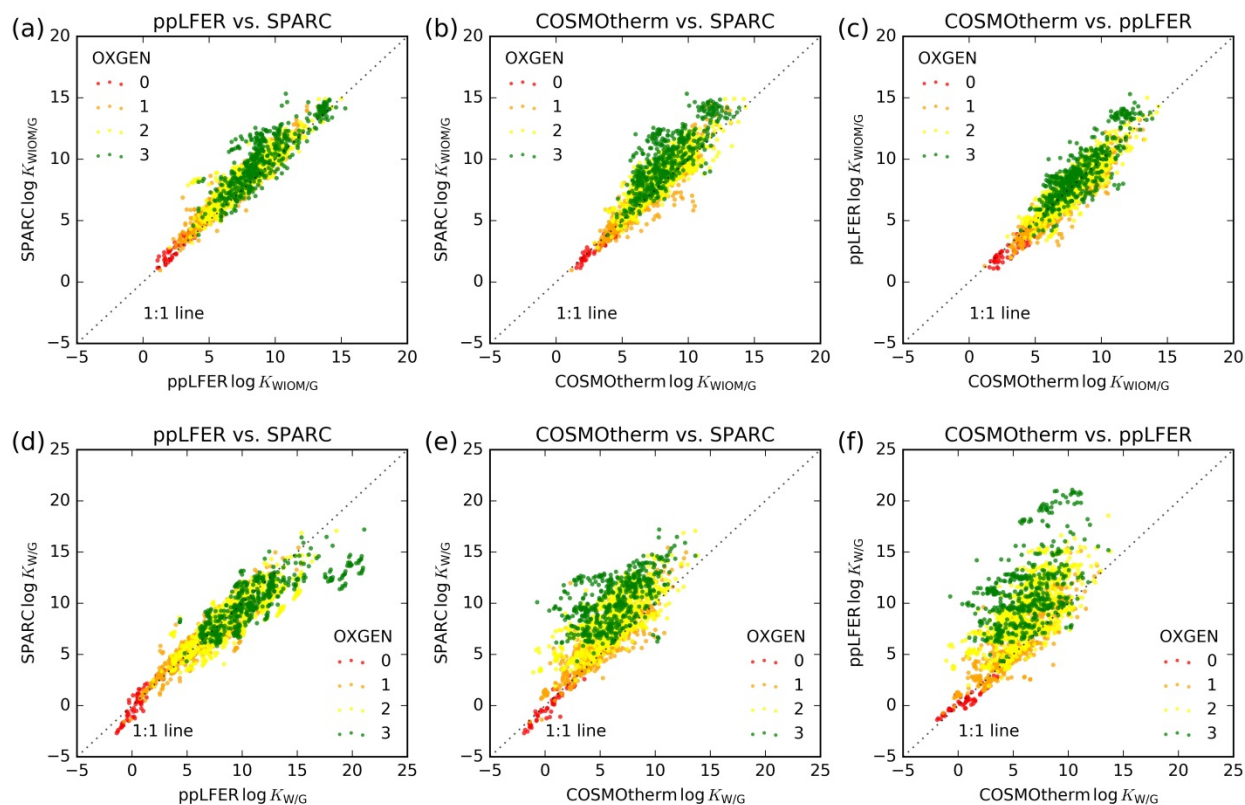


**Figure S7** Comparison of the  $K_{WIOM/G}$  (upper panel) and  $K_{W/G}$  (lower panel) predicted using COSMOtherm, SPARC and ppLFERs. The color scale indicates the generation of oxidation of the molecules. The oxidation generation information is available for 2148 compounds among all. Compound with an oxidation generation of 0 (i.e., OXGEN=0, the red dots) are precursor compounds.



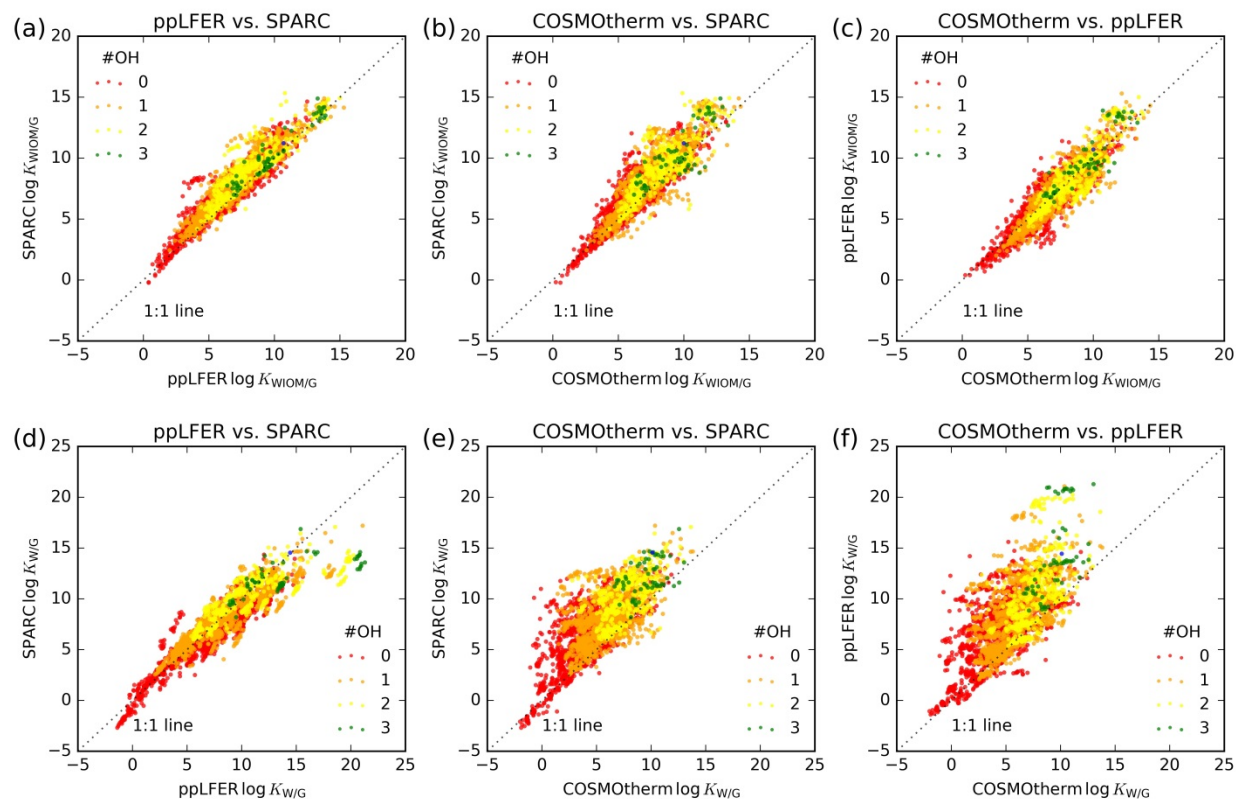


**Figure S8** Comparison of the  $K_{WIOM/G}$  (upper panel) and  $K_{W/G}$  (lower panel) predicted using COSMOtherm, SPARC and ppLFERs. The color scale indicates the number of OH in the molecules.

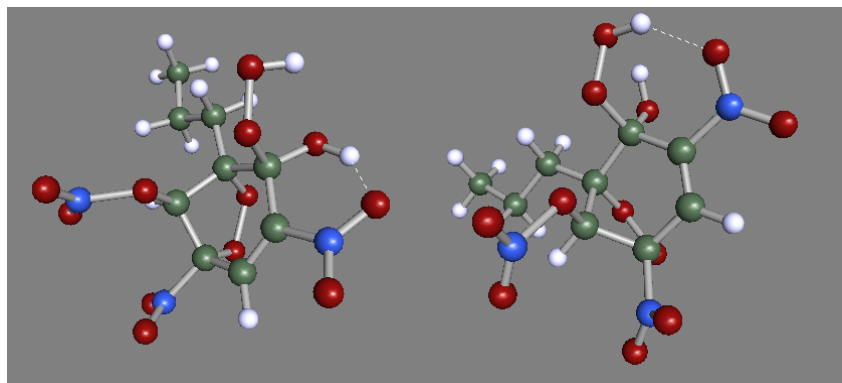


**Figure S9** Two conformers for an organic compound (MCM ID: NDNPBZLOOH). COSMOconf calculated six conformers for this compound and two are shown here as an example of intra-molecular interactions.

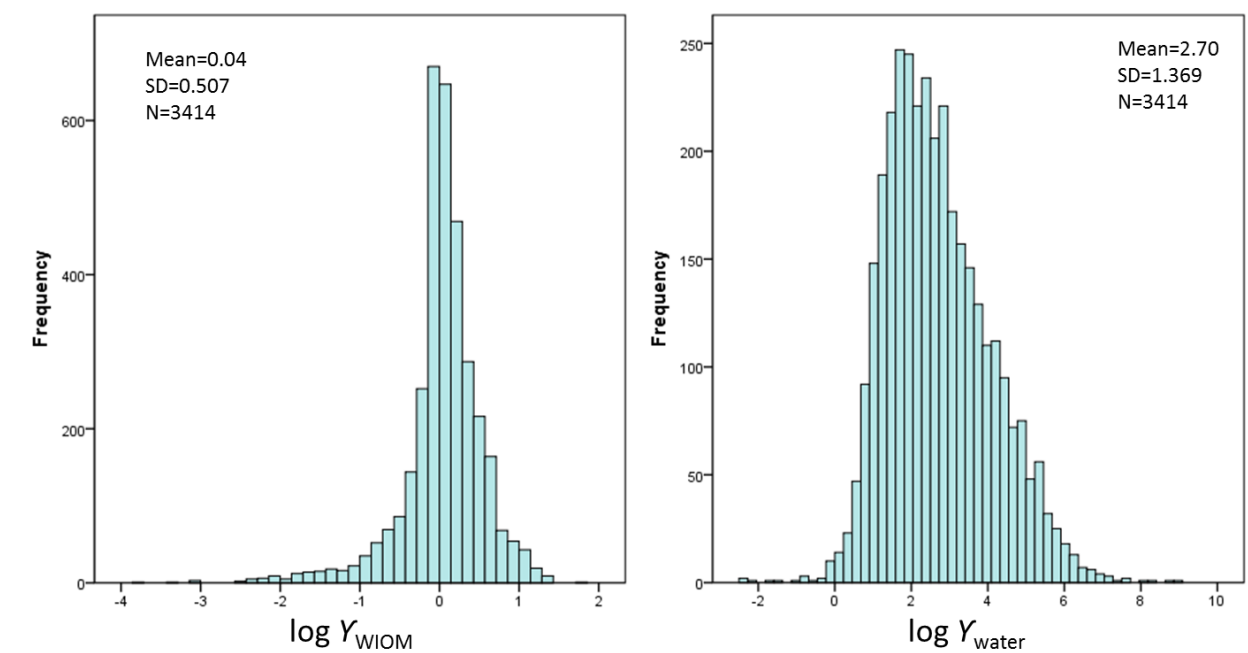


**Figure S10** Histogram of  $\log Y_{WIOM}$  and  $\log Y_{water}$  for 3414 organic compounds.

## Description of the Partitioning Space

Figure S11 are chemical partitioning space maps, showing the combinations of partitioning properties that lead to dominant equilibrium partitioning to the gas (pink), aqueous (blue), and water insoluble organic matter phases (green), respectively. Four scenarios are assessed, with panel (a) representing an aerosol scenario (LWC  $10 \mu\text{g}/\text{m}^3$ ,  $10 \mu\text{g}/\text{m}^3$  OM), (b) representing a cloud scenario (LWC  $0.3 \text{ g}/\text{m}^3$ ,  $10 \mu\text{g}/\text{m}^3$  OM), (c) representing an aerosol scenario without a separated aqueous phase (LWC  $0 \mu\text{g}/\text{m}^3$ ,  $10 \mu\text{g}/\text{m}^3$  OM) and (d) representing a cloud scenario without a separated WIOM phase (LWC  $0.3 \text{ g}/\text{m}^3$ ,  $0 \mu\text{g}/\text{m}^3$  OM). The dotted lines in the space indicate boundaries for different fractions of compounds in each phase. For instance, a compound with a  $\log K_{\text{W/G}}$  of 11 and a  $\log K_{\text{WIOM/G}}$  less than 10 (i.e. on the boundary line between the light pink and light blue region) would have 50 % each in either the gas or aqueous phase. The white color triangle in (a) and (b) shows the transition region where less than 50 % are present in each of the three phases.

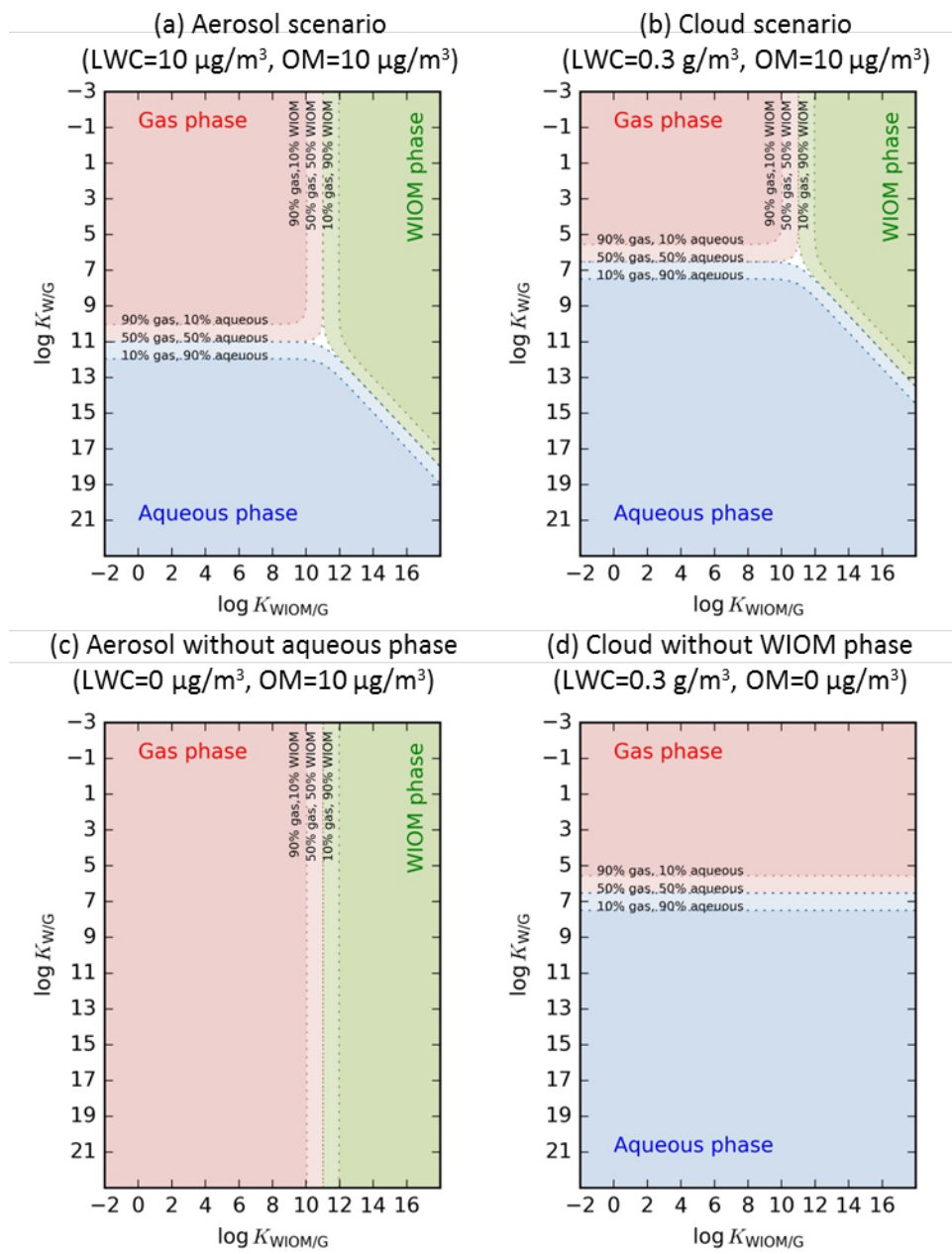


**Figure S11** Partitioning space map for aerosol (a), cloud (b), aerosol without aqueous phase (c) and cloud without WIOM phase (d)

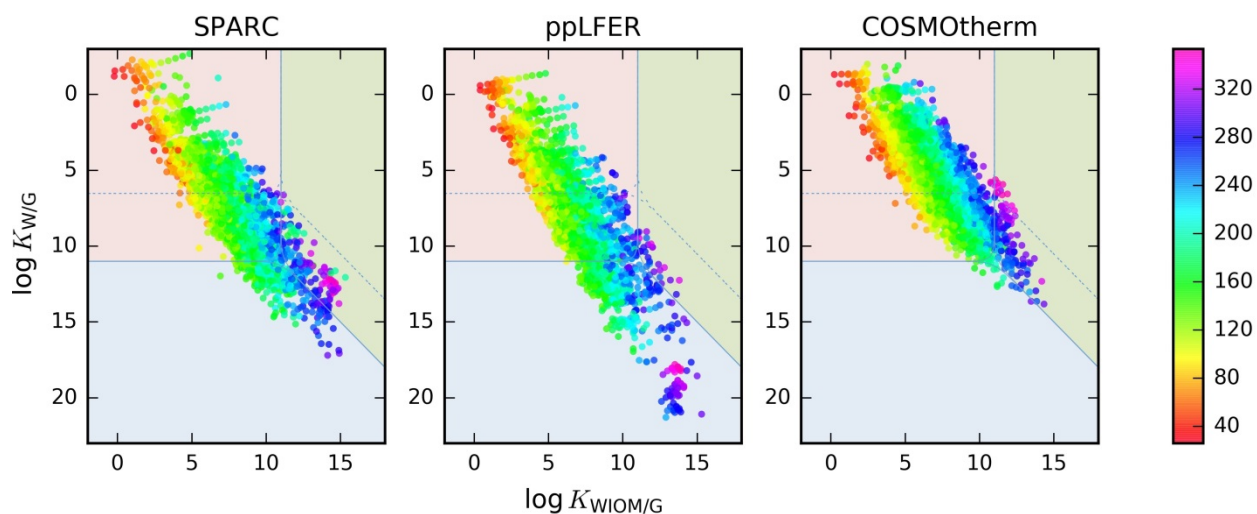


**Figure S12** Partitioning space plot, showing in pink, blue and green the combinations of partitioning properties that lead to dominant equilibrium partitioning to the gas, aqueous and WIOM phases, respectively. The solid and dotted lines are boundaries for an aerosol scenario (LWC  $10 \mu\text{g}/\text{m}^3$ ,  $10 \mu\text{g}/\text{m}^3$  OM) and a cloud scenario (LWC  $0.3 \text{ g}/\text{m}^3$ ,  $10 \mu\text{g}/\text{m}^3$  OM), respectively. The color scale indicates the molecular mass of the molecules.

## References

Donahue, N. M., Robinson, A. L., Stanier, C. O., and Pandis, S. N.: Coupled partitioning, dilution, and chemical aging of semivolatile organics, *Environmental Science & Technology*, 40, 2635-2643, 10.1021/es052297c, 2006.